https://doi.org/10.33271/nvngu/2022-6/059

Taleb Hosni Abderrahmane[*1,2],
orcid.org/0000-0001-8942-9492,
Guemidi Ismahene[1,3],
orcid.org/0000-0002-0486-9622

1 – FIMAS Laboratory, University of Bechar, Algeria
2 – Department of Civil Engineering and Hydraulic, Institute of Science and Technology, University Center of Mila, Mila, Algeria
3 – University Chadli Bendjedid, El Tarf, Algeria
* Corresponding author e-mail: talebhosni@yahoo.fr

THE INFLUENCE OF FISSURED MATERIAL ON TUNNEL STABILITY (A NUMERICAL STUDY)

Purpose. To understand the effect of fissured material on tunnels. These infrastructure tunnels must be safe in all respects, including construction, materials, and more. One of the challenges which engineers face is the need to consider material types as well as fissured material. As a result, in order to ensure the safety of the tunnel, it is important for us to anticipate possible precipitation, displacements, stresses and strains caused by the construction of tunnels in fractured environments.

Methodology. The OPTUMG2 software was used for this numerical study, the tunnel was modeled applying the hypothesis of two-dimensional plane deformation with the use of the finite element method, which is used to model continuous media. The Mohr-Coulomb criterium was considered to simulate the elastoplastic nonlinear behaviour of this model.

Findings. The findings demonstrate that the orientation of weakness planes can have a major impact on tunnel stability. Thus, it was observed that 45, and 60° for angle α_1, and 110, and 135° for the second angle α_2 present the most critical situations. The influence of fissured material (soil) on civil engineering projects such as tunneling should be taken into consideration.

Originality. The tunnel's stability is determined by the measuring of the displacement (settlement), stresses, and deformation, under the effect of the fissured material in the environment. In this paper we simulated a model with various crack angles. As for the orientation of plane, for the angl3e α_1 the values are changed to 0, 20, 45, 65, and 90°, the second angle α_2 was changed from 110, 135, 155, 175, to 180°.

Practical value. The number of tunnels and infrastructure projects is constantly increasing. This is because they are important for the development of countries and for accelerating economic growth, shortening distances and travel time by linking urban areas that have natural obstacles such as mountains. We found that the orientation planes can have a major impact on tunnel stability. Thus, it was observed that 45, and 60° for first angle, and 110, and 135° for the second angle present the most critical situations.

Keywords: *modelling of tunnel, fissured material, finite element method, settlement of soil, OPTUMG2 software*

Introduction. The rapid population growth includes the establishment of new towns and urban areas, as well as the development of transportation methods such as bridges, roads, and underground transportation systems like tunnels, which have become an essential part of metro cities; they play an important role in a country's growth.

Tunnelling has long been regarded as an art form, requiring engineers and builders to acknowledge and cope with the uncertainty of variable ground conditions (geotechnical and geological). The designers encounter a variety of obstacles, mostly associated with the security of workers during construction activities; the excavation-provoked settlements; the face and the cavity must be stable, as well as the end product quality; the viability of the building process is thus heavily influenced by the hydro-mechanical behaviour of excavated mass (soils and rock) [1].

The tunnelling may be divided into three steps conceptually: firstly, planning (feasibility analysis), which identifies the limits and risks of the project, with outlining and giving a rough design for the tunnel; secondly, engineering, devoted to the creation of precise and construction-ready designs; finally, building, execution, and ultimate update of the tunnel's preconstruction design, as well as the maintenance plan [1]. Tunnelling has seen several technological advancements as a result of the vast number of demanding infrastructure measures implemented over recent years. For tunnelling, the methods and technology are determined by the situation, the tunnel's use, location, geotechnics, geology, length, shape, diameter, groundwater levels, and available materials, among other factors. There is a variety of tunneling construction methods [2, 3], among these are: Cut and Cover Method (Bottom Up; Top Down); Drill and Blast Method (New Austrian Tunnelling Method); Tunnel Boring Machine Method (Slurry TBM, Earth Pressure Balance, Variable Density Tunnel Boring Machine); and Jacked Box Method.

The tunnels may be studied using different experimental, analytical, and numerical methods. Because of better computer efficiency, the numerical technique is commonly used to analyze tunneling problems for various properties and different loading types [4–8].

In tunnel stability analysis, numerical methods such as the finite element method (FEM), finite difference method (FDM), and discrete element method (DEM) have been frequently employed [9]. Previous to 2000, Negro and Queiroz [10], and Muniz de Farias, et al. [11] provided an overview of the finite-element method utilized for tunneling investigations. After reviewing more than 65 published research, they discovered that the finite element method (FEM) is the most prevalent method, accounting for 96 percent of the published examples. They also pointed out that 92 percent of the published assessments were still done in 2D, with assumed plane strain conditions. Another interesting finding was that most assessments continue to use elastic-perfectly plastic models [12].

In the study on tunnels, 3D FEM has shown to be an essential method of analysis [13, 14] along with a stability analysis for an existing tunnel-support system for a crossing tunnel and determined that local thickening is required for the current tunnel's stability. The FEM analysis is a useful means for analyzing tunnels and deep excavations [15, 16].

Zaid M. [17] used 3D FEM to investigate the stability of tunnels under the effects of loading on rock tunnels, with different areas constructed to differing unconfined compressive strengths. In another paper, the simulation of lined and unlined tunnels under static loading conditions was carried out by 3D FEM using different rock types and with diverse stages of rock weathering. The author determined that rock weathering and overburden depth have a significant impact on tunnel stability [18]. Md. Rehan Sadique, et al. [19] carried out numerical analysis by using Abaqus software. The 3D FEM was used for the simulation of the effect of internal blast loading in rock tunnels with three types of rock. They obtained the following results: stress, strain energy, damage, shock wave ve-

locity, deformation, shock wave velocity, pressure, and acceleration. In another research work, the analysis of rock tunnels having a shear zone was subjected to internal blast loading. Many shear zone orientations of angles were exposed, with respect to the tunnel axis being considered to see their effect. In this study, they discovered that the most dangerous situation is when shear sections are oriented at 60° [20]. A three-dimensional FEM nonlinear elastoplastic is used to model the reinforced concrete lining when exposed to impact loading with three stages of rock weathering. They have analyzed the extent of deformation and damage in the tunnel by four different explosive device weights and the greatest penetration in the rock at the moment it hits the tunnel surface. They concluded that the reinforced concrete lining suffers severe compression and tension damage at the tunnel's crown and that this damage is concentrated in the middle one-third of the tunnel's length, regardless of the explosive device's weight shift [21]. The 3D Finite element method was used to model the Tunnel with Abaqus software. They used the nonlinear elastoplastic material models for the different constitutive material models, for concrete, reinforcement, rock, inside-air of the tunnel, and trinitrotoluene (TNT). In connection with the blast impact, the behaviour of adjacent rock, as well as weathering, has been researched. In the event of blasting, a gradual deformation was seen from fresh granite to highly weathered granites, passing through slightly and moderately weathered granites. They also observed that the behavior of highly weathered rock was unusual, and it failed terribly [22]. The authors M. Zaid, et al. [23] used 3D finite element method to analyze the tunnels of Himalayan mountains with three types of rock. This research is related to the effect of varied overburden pressure and the lining thickness under static and surface blast loading, they also changed the shape of the tunnel (four shapes). According to the research, they concluded that the circular form is the safest tunnel among the other forms. On the other hand, the arch tunnel gives the most resistance under blast loading conditions. DEM modeling, among the several numerical methods, has recently gained use in tunnel engineering, Wang, et al. [24] investigated the stress responses of dry granular ground to shield-driven tunnels, and these researchers created a 2D DEM model.

Some research studies show instances of geotechnical engineering analysis of fissured materials utilizing the limit analysis approach, to analyze the bearing capacity of shallow foundations. Among them, are Davis (1980), Alehossein, et al. (1992), Lav, et al. (1995), and Zheng, et al. (1997). Almost all of the researchers came to the same conclusion that the carrying capacity of these foundations is greatly reduced by the presence of weak fissures and joints. After these research studies, Zheng, et al. [25], came and presented their research to develop a generic numerical method for determining the lower bound and upper bound solutions to the bearing capacity of a smooth or rough rigid strip footing on fissured soil or rock using the limit analysis method. Most past research used the fissured material for simulating the bearing capacity of shallow foundations; they did not use this material (fissured material) to analyze the tunnels. In this paper we try to study the effect of fissured material on the tunnel.

Fissured material. Concerning the fissured soil (Fig. 1), it is possible to account for the strength of materials having regular fissure patterns, by taking on a grouping of the Mohr-Coulomb criterion model with additional constraints on shear and normal stresses on fissure surfaces [26]. The two fissure planes can be defined so that the strength is restricted by

$$F(\sigma) \le 0,$$

where F is the usual function of the Mohr-Coulomb criterion

$$|\tau_1| + \sigma_1 \tan\varphi_1 - c_1 \le 0, \quad \sigma_1 \le k_{t1};$$

$$|\tau_2| + \sigma_2 \tan\varphi_2 - c_2 \le 0, \quad \sigma_2 \le k_{t2},$$

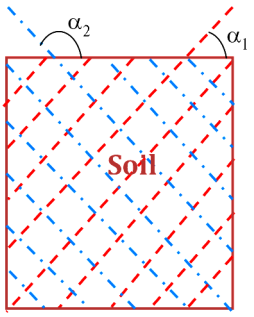

Fig. 1. Fissured soil

where (σ_1, σ_2) are the normal stresses and (τ_1, τ_2) are the shear stresses on the fissure planes (α_1, α_2). In addition, k_{ti} is tensile strength of plane; c_i is the cohesion on Plane i; φ_i, is the friction angle on Plane i; α_i is orientation of plane.

Davis (1980), Zheng, et al. (1997), and Zheng, at al. [25], have already discussed the developments of failure criteria for materials having regular sets of fissures. This study aims to examine the stability of a tunnel in fissured soil using the finite element method.

Numerical study. ***Geometry and Materials.*** Fig. 2 demonstrates the model's geometry. The finite element method was used with 2D plane strain conditions, by using OPTUMG2 software. The entire modeling domain's width is 110 meters, and its height is 52 meters. The diameter of the tunnel is 8 meters, and it has an overburden depth of 24 m. The boundary condition has fixed support at the base, and the vertical sides have roller support. For meshing, a 6-node Gauss (1) element was used (triangular or arbitrary shape), and surrounding the tunnel, the mesh size has been refined. Fig. 2, *b*. In this study, the Mohr-Coulomb criterion (2) was used to simulate the elastoplastic behavior (3) of soil (one layer), and the concrete of the lining (thickness = 0.25 m). Table 1 shows the parameters of the soil, concrete lining, and fissured material.

Table 1 lists the modeling characteristics of soil, fissured soil, and concrete lining utilized in our models.

Modeling phases. The modeling in this study can be subdivided into three phases (steps). The first phase is the calculation of the initial stress state. In this stage, the condition takes into account the impact of vertical stress on the depth gradient under gravity's influence. The tunnel is excavated in the sec-

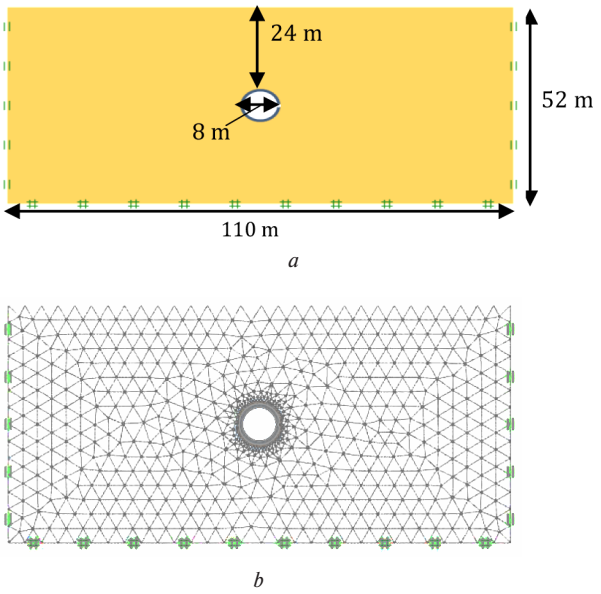

Fig. 2. The geometry (a), Mesh and Boundary condition (b), of the tunnel

Table 1

The properties of the soil, fissured material, and concert lining

SOIL PROPERTIES	Symbol (unite)	Value
Young's modulus	E (MPa)	43.4
Poisson's ratio	ϑ	0.26
Friction angle	φ (°)	29.5
Cohesion	c (kPa)	39.5
Saturated density	γ_{sat} (kN/m^3)	20.5
FISSURED MATERIAL		
Orientation of plane	α_i (°)	There is a value for each α_i
Cohesion on the plane	c_i (kPa)	0
Friction angle on the plane	φi (°)	20
Tensile strength of the plane	k_{ti} (kPa)	Infinity
CONCRETE LINING		
Thickness	(cm)	25
Weight	W (kg/m/m)	625
Section area	A (cm^2/m)	2500
Moment of inertia	I (cm^4/m)	$1.302 \cdot 10^5$
Plastic section modules	S (cm^3/m)	$1.563 \cdot 10^4$
Young's module	E (MPa)	$2.54 \cdot 10^4$
Yield strength		28

ond phase, and the tunnel wall (perimeter) is given a relaxation ratio which allows for a corresponding reduction in the stresses on the excavations completely supported in this step, with a relaxation ratio of 0.3. The tunnel boundary support (concrete lining) was installed in the last phase.

The task of this concrete lining is to preserve or improve the tunnel's safety.

Results and discussion. In this numerical model, we want to assess the vertical and horizontal displacements at the ground surface level ($Y = 52$ m), and near the tunnel at 30.5 and 21.5 m. Fig. 3 shows the Y heights (52, 30.5, 21.5 m) of the numerical model. The analysis was carried out with three different numerical cases. The first instance involves modeling intact material (soil without fissured material); the second numerical case involves modeling fissured material with different α_1, and the last case involves modeling with various angles of α_2.

Vertical and horizontal displacements (Intact Material). As a result, the design engineer must pay close attention to the details. In the first case, we modeled this tunnel without any fissured material. The aim is to measure the vertical and horizontal displacement along with the selected profiles $Y = 52$, 30.5 m, and $Y = 21.5$ m.

Fig. 4, *b*, depicts the tunnel's final surface settling curves ($Y = 52$, 30.5 m) following excavation, the maximum surface settlement value is 6 cm above the tunnel ($Y = 30.5$ m), with a settlement trough width of 19 m derived by fitting observed

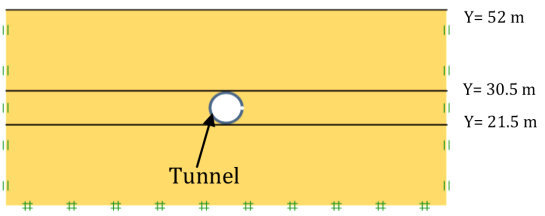

Fig. 3. The tunnel's transverse section and its location in the section studied

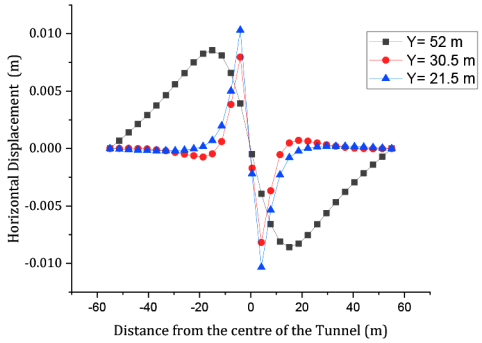

a

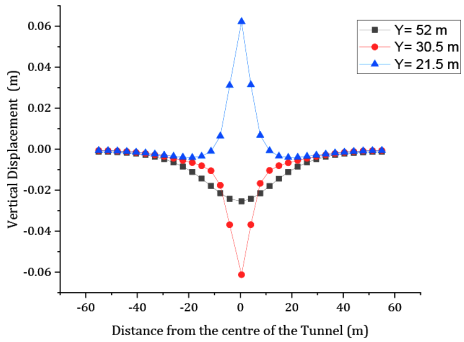

b

Fig. 4. Horizontal (a); Vertical displacement (b)

data. At the ground surface level $Y = 52$ m, the settlement is 2 cm, but the displacement of soil under the tunnel ($Y = 21.5$ m) has the same results at 6 cm but against the settlement in the direction of the tunnel void (the vertical direction).

On the other hand, the horizontal displacements are presented in Fig. 4, *a*. The greatest horizontal displacement amount occurred at the center of the profile tunnel (below the tunnel by 1 cm) with a value of 1 cm. It is worth noticing that the displacements are practically at the tall surface profile ($Y = 52$ m, at the ground's surface), albeit with minor variations. The displacements will expand in the center of the model, with slight displacements on the sides.

As shown in Fig. 5, the vertical and horizontal displacements are represented on a color scale for the unit meter. The distribution of the soil displacements is caused by tunnel excavation. It is observed that the vertical displacements of the soil (Fig. 5, *a*) and concrete lining (Fig. 7, *a*) are found to be symmetrical in relation to the tunnel's vertical axis; the top and the tunnel's base have the largest vertical displacements Figs. 5, *a*, *b*.

The stability study was carried out by looking at the deformation at the lining interface and soil mass. Fig. 5 shows that the deformations are more developed at the top of the tunnel than at the lower part. There are fewer deformations on the tunnel's left and right sides.

The maximum horizontal displacements occur on the free surface on both the left and right sides of the tunnel. We have also observed an asymmetry of the horizontal displacements (Fig. 6, *b*). Fig. 6, *b*, illustrates that the left side of the tunnel has positive displacements (a shade of red color), while the right side has negative displacements. They correspond to a tendency for horizontal convergence of the ground towards the center of the tunnel. The vertical displacement of soil (0.068 m) is greater than the horizontal displacement of soil (0.0304 m). The difference is about 50 %.

We can see the deformation at the tunnel's perimeter more clearly (Fig. 7). The deformations occur in the lining due to soil pressure, and the development of surface settlement might indicate the failure zone that develops around the tunnel. With a value of ∓5.1 mm, the horizontal displacements are the same on both sides of the structure's concrete

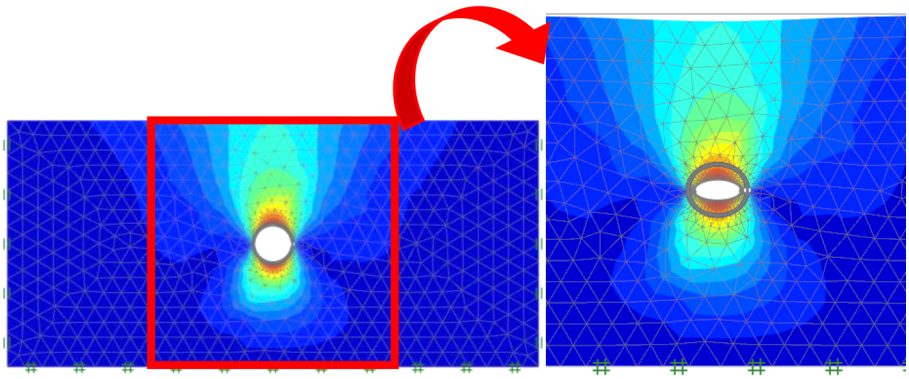

a *b*

Fig. 5. Deformation of soil (a); concrete lining (b)

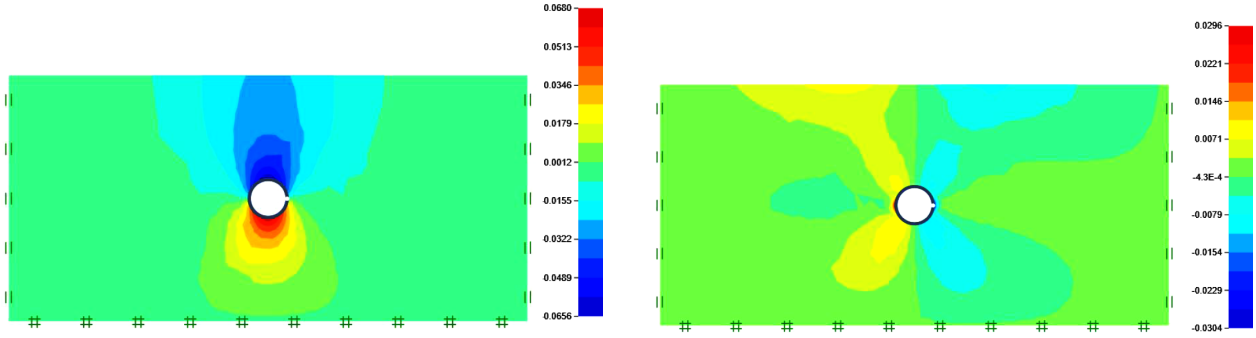

a *b*

Fig. 6. Displacements (m): Vertical (a); Horizontal (b)

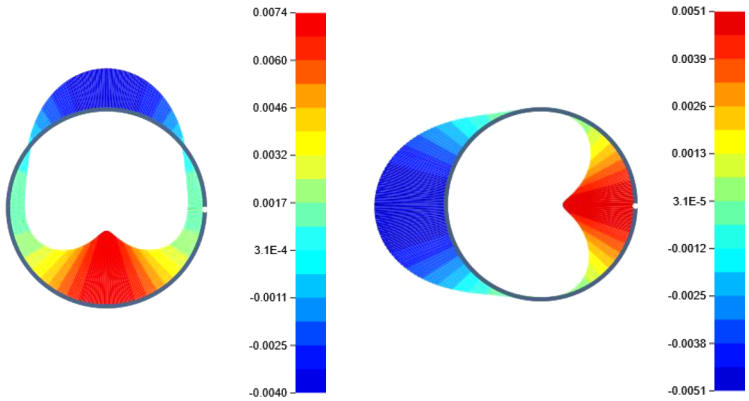

a *b*

Fig. 7. Concrete lining displacements (m): Vertical (a); Horizontal (b)

lining. On the other hand, the vertical displacements are different. The maximum displacement (7.4 mm) occurs beneath the tunnel, while the minimum displacement occurs at the tunnel's top (–4 mm).

The areas of soil are naturally stressed by digging the tunnel. Fig. 8 shows the development of stress contours after the phase of lining concrete for the tunnel, which have a maximum stress value of ∓217.216 kPa at the right and left of the tunnel surrounding the lining tunnel.

We observe that all the vertical stresses are negative with a value of –1069.5 kPa, which corresponds to compressions. The vertical stresses in the model located just above the tunnel and below the apron are almost non-existent with a value of 0.185 kPa. The vertical stress concentration is more or less well developed at the left and right lining concrete of the tunnel. The vertical stress distribution is symmetrical with regard to the tunnel's vertical axis, as seen in Fig. 8, *a*.

Fig. 8 shows that the horizontal stress distribution is almost symmetrical to the vertical axis of the tunnel. The horizontal stresses on the right and left concrete lining of the tunnel are almost zero (a shade of red color). The horizontal stresses at the top and at under the concrete lining of the tunnel are greater than the left- and right-side stresses.

In order to better visualize the soil's influence on the concrete lining, Fig. 9 shows that the ground movements caused by excavation can produce shear, normal forces, and bending moments around the concrete lining of the tunnel due to the displacements and pressure of the soil.

Fig. 9, *c*, illustrates the shear force contour of lining concrete, which has a maximum value of 23.608 kN, is directed toward the tunnel's center.

Due to the pressure of soil surrounding the lining tunnel, the distribution bending moment and the normal forces are symmetrical with regard to the tunnel's vertical axis, as seen in Figs. 9, *a*, *b*.

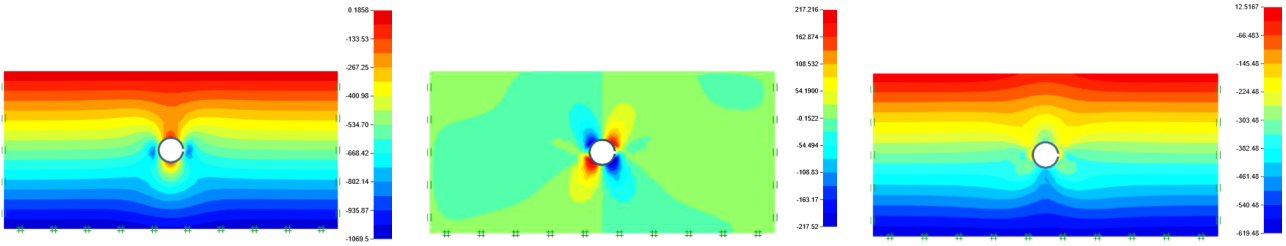

a *b* *c*

Fig. 8. Vertical stress (kPa) (a); Shear stress (kPa) (b); Horizontal stress (kPa) (c)

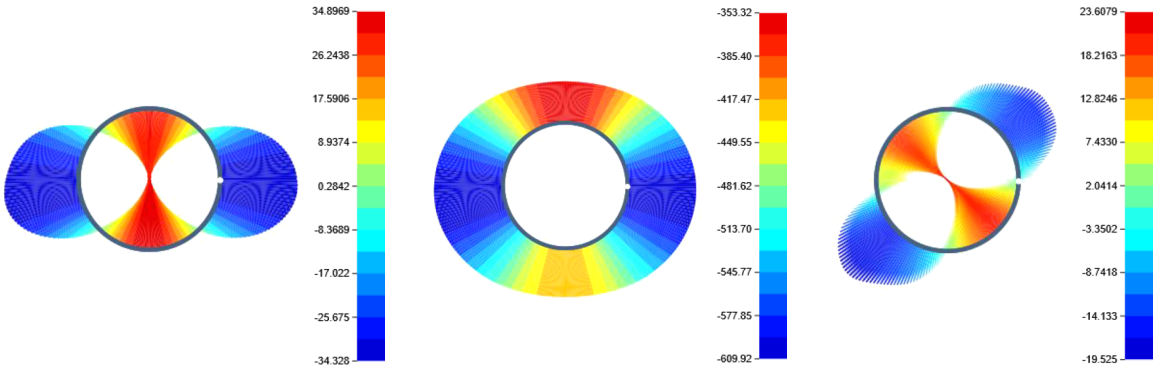

a *b* *c*

Fig. 9. Bending Moment (kN/m) (a); Normal Force (kN/m) (b); Shear Force (kN/m) (c)

We observe that the bending moment values of 34.897 kN · m are almost the same at the top and bottom of the tunnel, with the right and left sides.

We saw that all of the normal force values were negative. It is clear that the soil pressure on the structural lining has a major impact and indicates compression on the lining concrete. The normal force value on the top is –353.32 kN, which is nearly 50 % lower than the normal force value on the right and left sides (–609.92 kN).

Parametric study on the tunnel with the presence of a fissured material. Tunnel modeling requires accurate prediction of the deformation response of the ground surface settlement, displacements, deformations of concrete lining, and shear stresses. This section examines the tunnel under fissured material with different angle values.

The tunnel's stability is determined by measuring the displacement (settlement) and deformation of fissured material from various angles (α_1; α_2). In this research, we used 10 angles: the first angle α_1 is changed by five values) 0, 20, 45, 65 and 90°). We modified the second angle α_2, with 5 fives values which are arranged as (110, 135, 155, 175 and 180°).

The effect of changing the angle α_1 on the soil. The greatest settlement amount occurred at the center of the profile tunnel. At the level of the ground surface ($Y = 52$ m), the maximum surface settlement is due to the angle of 65° with a value of 9.3 cm (Fig. 10, *a*). In $Y = 30.5$ m, we have also the same displacement (9.3 cm) but in this case, the maximum displacements are resulting from the angles of (45 and 90°). Fig. 10, *b*, shows the value of the settlements. At the bottom of the tunnel ($Y = 21.5$ m), Fig. 10, *c*, the vertical displacements are presented going towards the vacuum in the tunnel's center and all the values of the different angles are almost the same results (7.5 cm), with a slight settlement (1 cm) on the left and right of the tunnel.

At the level of $Y = 30.5$ m (near the tunnel), the biggest horizontal displacement (±3.6 cm) amount happened in the profile tunnel's center with the 45° angle on the left, with the 65° on the right side of the tunnel. Level of the ground surface ($Y = 52$ m), the horizontal displacements (±2.3 cm) are smaller when we compared to $Y = 30.5$ m.

When we compared the horizontal displacement at the bottom of the tunnel ($Y = 21.5$ m) with other levels ($Y = 52$ and 32.5 m), we found that it is smaller with a value (±2 cm) than the results of other levels. Fig. 11, *c*, shows the horizontal displacement of the angle 45° to the right and the other (65°) to the left side of the tunnel's center.

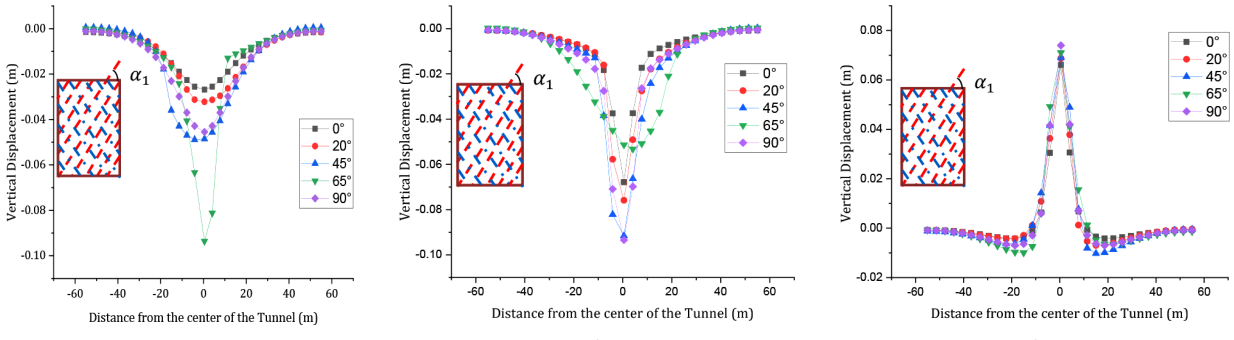

a *b* *b*

Fig. 10. Vertical displacements for various α_1:
a – Y = 52 m; b – Y = 30.5 m; c – Y = 21.5 m

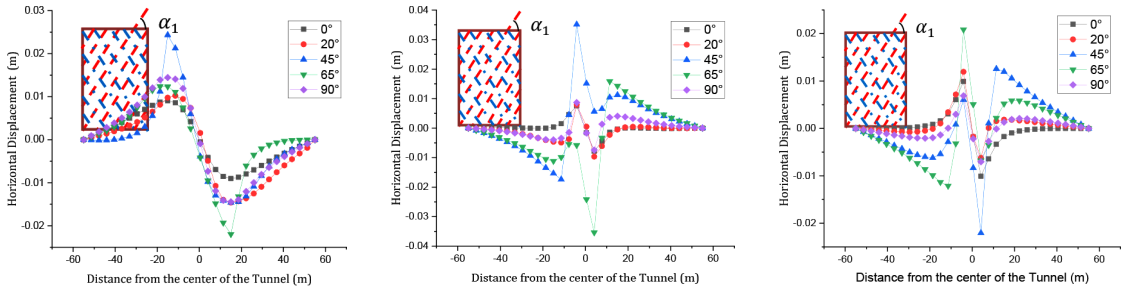

a *b* *c*

Fig. 11. Horizontal displacements for various α_1:
a – Y = 52 m; b – Y = 30.5 m; c – Y = 21.5 m

The following table summarizes what is happening around the tunnel under the effect of the orientation plane change of α_1.

The results of the numerical study on the tunnel precisely around the concrete lining provided the following points for different angles α_1 (Table 2):

1. For α_1 (45°), we have a maximum bending moment of 48.692 kN · m/m and the highest normal force is 644.927 kN/m (compression).

2. The maximal shear force is 36.5227 kN/m, corresponding to 65°.

As we saw in the graphs (Figs. 10, 11), vertical and horizontal displacements are caused by fissured material (α_1). In this arrangement, angles 45 and 65° have the largest influence.

Fig. 12 presented the distribution of shear stresses of α_1. The shear stresses are concentrated around the tunnel due to the excavation phase; we noticed that the general shape of this distribution of shear stresses is almost the same at all angles. But there is little change in the magnitude of this distribution. The biggest value is 219.674 kPa, which is due to the effect of the angle of 65°, and the smallest value is 180.64 kPa, due to the angle (20°).

The effect of changing the angle α_2 on the soil. In the last part of this numerical study, we will analyze the effect of angle α_2 in the same way as we treated angle α_1, in terms of displacements vertically and horizontally.

The highest amount of surface settling happened in the tunnel's profile center (vertical axis). At ground level (Y = = 52 m), the largest surface settlement is due to an angle of 110° with a value of 5.7 cm (Fig. 13, *a*). We have a displacement of 9.8 cm at Y = 30.5 m; however, the maximal displacement is caused by the angles of 110 and 135°, in this case the worth of the settlements is depicted in Fig. 13, *b*.

Fig. 13, *c* shows the vertical displacements flowing towards the void in the tunnel's center at the bottom of the tunnel (Y = = 21.5 m), and all of the angles' values are almost the same results (7.3 cm), with a minor settlement (1 cm) on both the left and right sides of the tunnel.

Fig. 14, *b* illustrates the horizontal displacement near the top of the tunnel at Y = 30.5 m. The maximum displacement amount occurred in the tunnel's profile center under the impact of the angle of 110° on the left, with a value of +3.8 cm. Due to the impact of the 135° angle, the height of horizontal displacement on the right side of the tunnel is –3.8 cm. Horizontal displacements are smaller at the ground surface (Y = 52 m) than at Y = 30.5 m, with a value of 1.8 cm (Fig. 14, *a*).

Table 2

Results of shear, normal forces, and bending moments of the concrete lining for each (α_1)

Angle (α_1)	0°		20°		45°		65°		90°	
	Maxi	Mini	Maxi	Mini	Maxi	Mini	Maxi	Mini	Maxi	Mini
Bending moment (kN · m/m)	37.1235	–37.1015	–40.037	37.7354	48.692	–41.904	–43.999	42.576	–40.790	32.335
Shear Force (kN/m)	34.86	–30.450	35.956	–22.959	27.220	–22.388	36.523	–22.944	33.150	–30.464
Normal Force (kN/m)	–622.593	–394.888	–630.69	–387.560	–644.927	–398.662	–640.292	–400.489	–629.780	–390.151

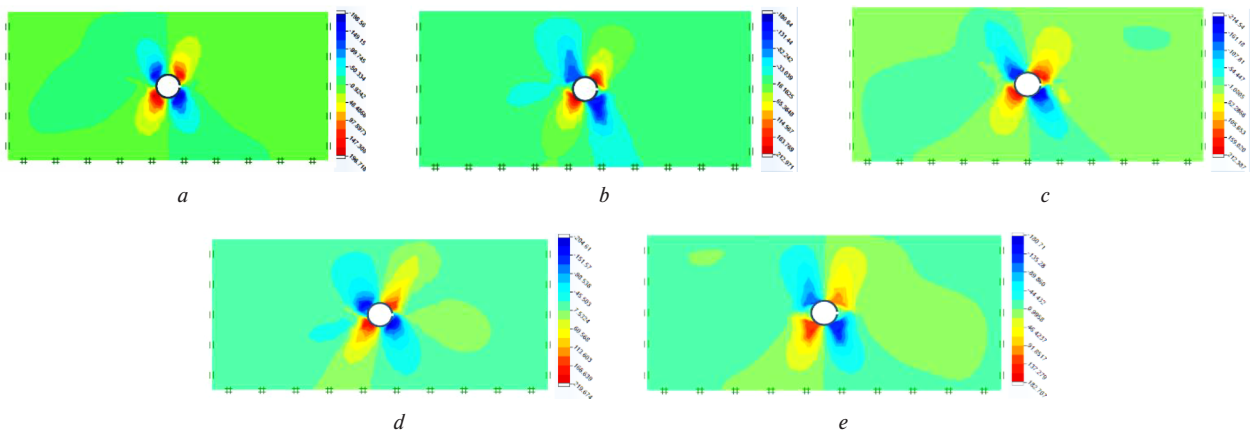

a *b* *c* *d* *e*

Fig. 12. Shear stresses of α_1:
a – $\alpha_1 = 0°$; *b –* $\alpha_1 = 20°$; *c –* $\alpha_1 = 45°$; *d –* $\alpha_1 = 65°$; *e –* $\alpha_1 = 90°$

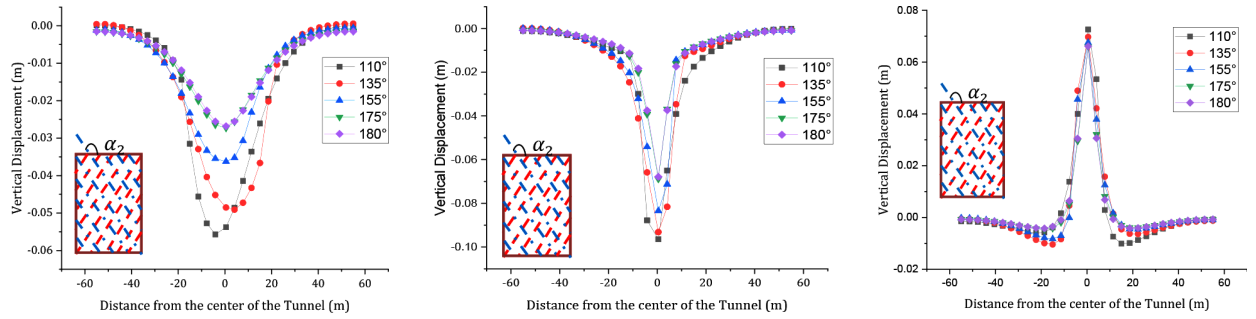

a *b* *c*

Fig. 13. Vertical displacements for various α_2:
a – Y = 52 m; b – Y = 30.5 m; c – Y = 21.5 m

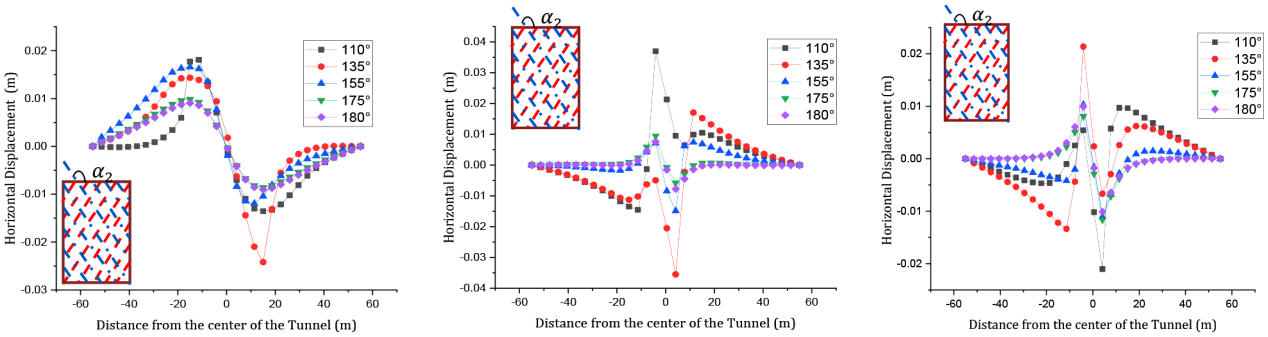

a *b* *c*

Fig. 14. Horizontal displacements for various α_2:
a – Y = 52 m; b – Y = 30.5 m; c – Y = 21.5 m

The maximal horizontal displacement at the bottom (Y = = 21.5 m) of the tunnel is ± 2 cm, it is lower than at the other two levels (Y = 52 and 32.5 m). Fig. 14, *c* depicts the reversal of events that occurred above the tunnel. The maximum horizontal displacements are presented under the effect of the angles 110° to the right and 135° to the left of the tunnel's center. As we have seen previously in the charts of vertical and horizontal displacements under the effect of fissured material (α_2).

Table 3 summarizes the results of bending moment, shear, and normal forces, for varied angles of α_2, the results of the numerical research on the tunnel precisely around the structure concrete lining provide the following information: The maximum shear force is 34.861 kN/m, which corresponds to a 180° angle. The greatest bending moment for α_2 (135°) is 49.980 kN · m/m, the maximal normal force is – 643.429 kN/m (compression). The results of the modeling for α_2 are congruent with what was found in α_1.

Fig. 15 presents the concentration of shear stresses of α_2 around the tunnel. The general shape of this distribution of shear stresses is almost the same at all angles. But there is little change in the magnitude of this distribution. The biggest value is 197.719 kPa, which is due to the effect of the angle (180°).

Summary results. The numerical results of settlement, vertical and horizontal displacements with two orientation planes (α_1, α_2), are summarized in these two Figs. 16, 17.

Fig. 16 shows the summary results of the settlements and vertical displacements of the tunnel with changes of α_1 and α_2.

Fig. 17 illustrates the results of the horizontal displacements of the tunnel with changes in α_1 and α_2. The essential results in this figure will be discussed at end of this paper.

The important points in these figures will be mentioned in the conclusion.

Conclusions. Geologically, there are many mountains in which tunnels can be built. The mountains consist of many types of soil and rock mass, including fissured materials. A two-dimensional finite element study has been carried out using the OptumG2 software to better understand how fissured materials behave in tunnels with changing orientation planes (α_1, and α_2). The displacements, settlements, deformation, and stress in the model are evaluated. The results clearly show that the distribution of displacements around the tunnel is similar in the two types of material. However, displacements in a fissured material are generally greater. We found that the maximum displacements are found at the tunnel's top and bottom (Y = 30.5 and 21.5 m, respectively). And the vertical

Table 3

Results of shear, normal forces, and bending moments of the concrete lining for various (α_2)

Angle (α_2)	110°		135°		155°		175°		180°	
	Maxi	Mini	Maxi	Mini	Maxi	Mini	Maxi	Mini	Maxi	Mini
Bending Moment (kN · m/m)	–41.873	38.881	49.980	–43.313	45.151	–40.725	38.472	–36.800	37.123	–37.101
Shear Force (kN/m)	–31.343	31.003	26.147	–23.557	29.844	–28.890	33.365	–30.950	34.861	–30.449
Normal Force (kN/m)	–642.583	–400.029	–643.429	–401.382	–636.270	–399.112	–622.903	–396.050	–622.593	–394.888

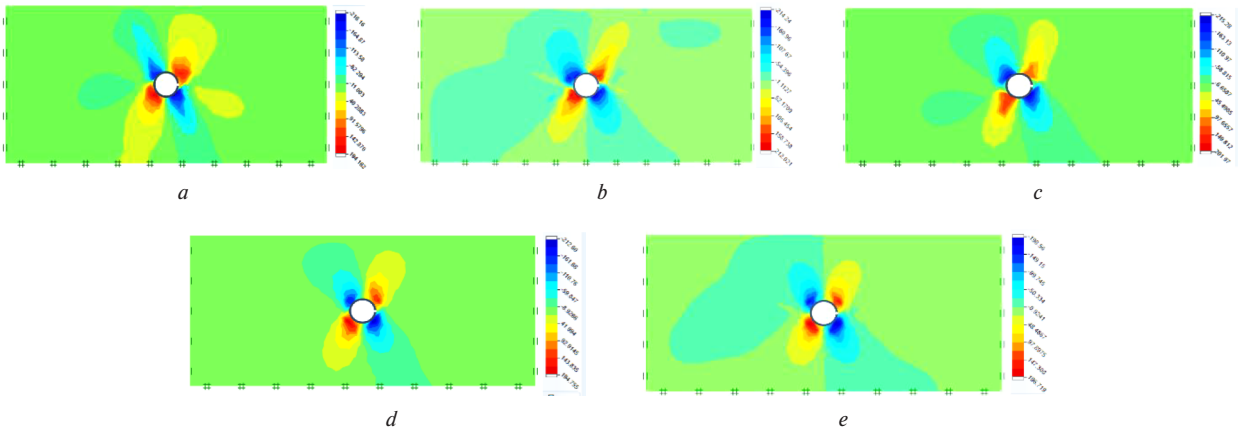

Fig. 15. Shear stresses of α_2:
a – $\alpha_1 = 110°$; *b* – $\alpha_1 = 135°$; *c* – $\alpha_1 = 155°$; *d* – $\alpha_1 = 175°$; *e* – $\alpha_1 = 180°$

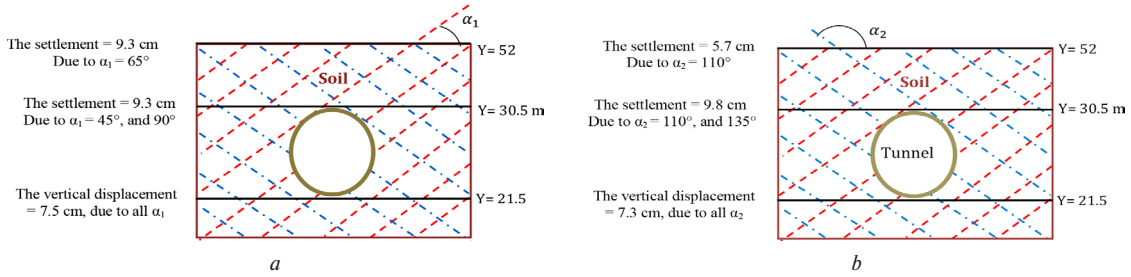

Fig. 16. Vertical displacement and settlement with α_1, *and* α_2 ($Y = 52, 30.5, 21.5$ *m*)

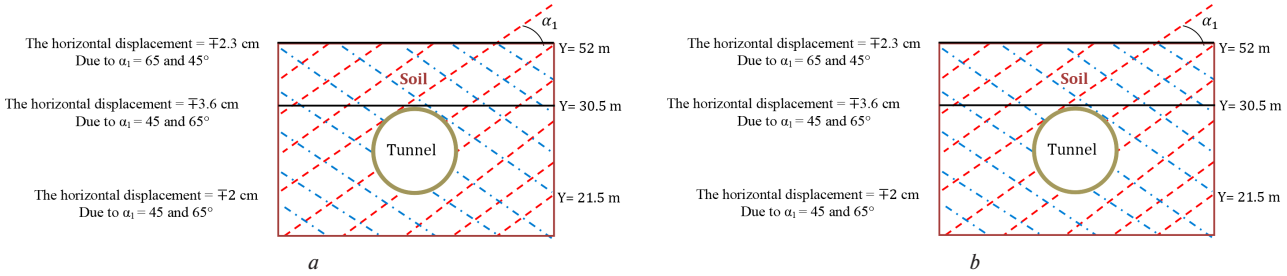

Fig. 17. Horizontal displacement with α_1, *and* α_2 ($Y = 52, 30.5, 21.5$ *m)*

displacement without fissured soil is significantly lower than the vertical displacement with fissured material, for instance ($Y = 52$ m), the surface settlement with an angle of 45° (9.2 cm) is 80 % bigger than the value of the surface settlement with intact material (2 cm). It is worth noticing that horizontal displacements are more evident at the tunnel level on both sides of the concrete lining. However, vertical displacements are much more important than horizontal ones. The largest displacements are usually seen near the tunnel's top and bottom. For example, when $Y = 30.5$ m the settlement is 9.3 cm, for a 45° angle, while the settlement of α_2 (110°) is 9.8 cm. The results clearly show that the maximum vertical and horizontal displacements are generally under the effect of the angles (45, 65°) for α_1, and the angles (110, 135°) for α_2. Finally, the OptumG2 software is well suited to calculating tunnels in fissured settings (for example, a fissured soil) that are exposed to static analysis, it solves problems from two different angles (orientations). We conclude that the influence of fissured soil is an important aspect in the design of civil engineering projects, such as tunneling.

Funding. *This research is carried out and funded in the context of the project "Interaction of geotechnical structures with their environments". Under the proposals "University Formation Research Project (PRFU)". The project approval code is: A01L02UN080120200002.*

References.

1. di Prisco, C., Peila, D., & Pigorini, A. (2022). *Handbook on Tunnels and Underground Works* (*I*st ed.). CRC Press. ISBN 9781003256175.

2. Athar, M. F., Zaid, M., & Sadique, Md. R. (2019). Stability of Different shapes of Tunnels in Weathering Stages of Basalt. In *Proceedings: National Conference on Advances in Structural Technologies (CoAST-2019), NIT Silchar.* India. Retrieved from http://www.nits.ac.in/conferences/CoAST_2019/CoAST_2019.html.

3. Khana, Z. A., Khana, Md. S., Sadiquea, M. R., Samantab, M., & Alama, M. M. (2021). Response of Twin Transportation Tunnel in Earthquake Loading: A Review 2021. *IOP Conference Series: Earth and Environmental Science*, 796, 012044. https://doi.org/10.1088/1755-1315/796/1/012044.

4. Shah, I. A., & Zaid, M. (2020). Behavior of Underground Tunnel under Strong Ground Motion. In *Proceedings of Indian Geotechnical conference 2020, December 17-19, 2020,* (pp. 229-239). Retrieved from https://www.researchgate.net/publication/348336923_Behavior_of_Underground_Tunnel_under_Strong_Ground_Motion.

5. Zaid, M., Irfan, S., & Farooqi, M. A. (2019). Effect of Cover Depth in Unlined Himalayan Tunnel: A Finite Element Approach. In *Proceeding of 8th Indian Rock conference, Indian International Centre, New Delhi, India, 03–04 March 2019,* (pp. 448-454). ISBN No. 81-86501-27-1.

6. Shahin, H. M., Nakai, T., Zhang, F., Kikumoto, M., & Nakahara, E. (2011). Behavior of ground and response of existing foundation due to tunneling. *Soils and foundations, 51*(3), 395-409.

7. Pakbaz, M.C., & Yareevand, A. (2005). 2-D analysis of circular tunnel against earthquake loading. *Tunnelling and Underground Space Technology, 20*(5), 411-417.
8. Mroueh, H., & Shahrour, I. (2003). A full 3-D finite element analysis of tunneling adjacent structures interaction. *Computers and Geotechnics, 30*(3), 245-253.
9. Hu, X., Fu, W., Wu, S., Fang, Yo., Wang, J., & He, Ch. (2021). Numerical study on the tunnel stability in granular soil using DEM virtual air bag model. *Acta Geotechnica, 16*, 3285-3300. https://doi.org/10.1007/s11440-020-01130-4.
10. Negro, A., & Queiroz, B.I.P. (2000). Prediction and performance of soft ground tunnels. In *Geotechnical aspects of underground construction in soft ground,* (pp. 409-418). Balkema, Tokyo, Japan.
11. Muniz de Farias, M., Junior, A.H.M., & Pacheco de Assis, A. (2004). Displacement control in tunnels excavated by the NATM: 3-D numerical simulations. *Tunnelling and Underground Space Technology, 19*(3), 283-293.
12. Do, N.-A., Dias, D., Oreste, P., & Djeran-Maigre, I. (2014). 2D Tunnel Numerical Investigation: The Influence of the Simplified Excavation Method on Tunnel Behaviour. *Geotechnical and Geological Engineering, 32*, 43-58.
13. Vermeer, P.A., Bonnier, P.G., & Möller, S.C. (2002). On a smart use of 3D-FEM in tunnelling. In *International symposium; 8th, Numerical models in geomechanics; NUMOG VIII,* (pp. 361-366).
14. Liu, H.Y., Small, J.C., Carter, J.P., & Williams, D.J. (2009). Effects of tunnelling on existing support systems of perpendicularly crossing tunnels. *Computers and Geotechnics, 36*(5), 880-894.
15. Nogueira, C.D.L., de Azevedo, R.F., & Zornberg, J.G. (2011). Validation of Coupled Simulation of Excavations in Saturated Clay: Camboinhas Case History. *International Journal of Geomechanics, 11*(3), 5622. https://doi.org/10.1061/(ASCE)GM.1943-5622.0000077.
16. Yang, F., Zhang, J., Zhao, L., & Yang, J. (2015). Upper-bound Finite Element Analysis of Stability of Tunnel Face Subjected to Surcharge Loading in Cohesive-frictional Soil. *KSCE Journal of Civil Engineering, 20*, 2270-2279.
17. Zaid, M. (2021). Dynamic stability analysis of rock tunnels subjected to impact loading with varying UCS. *Geomechanics and Engineering, 24*(6), 505-518. https://doi.org/10.12989/gae.2021.24.6.505.
18. Zaid, M. (2021). Three-dimensional finite element analysis of urban rock tunnel under static loading condition: Effect of the rock weathering. *Geomechanics and Engineering, 25*(2), 99-109. https://doi.org/10.12989/gae.2021.25.2.000.
19. Sadique, M.R., Zaid, M., & Alam, M.M. (2022). Rock Tunnel Performance Under Blast Loading Through Finite Element Analysis. *Geotechnical and Geological Engineering, 40*, 35-56. https://doi.org/10.1007/s10706-021-01879-9.
20. Zaid, M., Sadique, Md.R., Alam, M.M., & Samanta, M. (2020). Effect of Shear Zone on Dynamic Behaviour of Rock Tunnel Constructed in Highly Weathered Granite. *Geomechanics and Engineering, 23*(3), 245-59. https://doi.org/10.12989/GAE.2020.23.3.245.
21. Zaid, M. (2021). Preliminary Study to Understand the Effect of Impact Loading and Rock Weathering in Tunnel Constructed in Quartzite. *Geotechnical and Geological Engineering*. https://doi.org/10.1007/s10706-021-01948-z.
22. Zaid, M., Sadique, M.R., & Alam, M.M. (2022). Blast Resistant Analysis of Rock Tunnel Using Abaqus: Effect of Weathering. *Geotechnical and Geological Engineering*, *40*, 809-832. https://doi.org/10.1007/s10706-021-01927-4.
23. Zaid, M., & Shah, I.A. (2021). Numerical Analysis of Himalayan Rock Tunnels under Static and Blast Loading. *Geotechnical and Geological Engineering*, *39*, 5063-5083. https://doi.org/10.1007/s10706-021-01813-z.
24. Wang, S., Qu, T., Fang, Y., Fu, J., & Yang, J. (2019). Stress responses associated with earth pressure balance shield tunneling in dry granular ground using the discrete-element method. *International Journal of Geomechanics, 19*(7), 04019060. https://doi.org/10.1061/(ASCE)GM.1943-5622.0001434.
25. Zheng, X., Booker, J.R., & Carter, J.P. (2000). Limit analysis of the bearing capacity of fissured materials. *International Journal of Solids and Structures, 37*, 1211-1243.
26. Krabbenhoft, K., Lyamin, A., & Krabbenhoft, J. (2016). *Optum computational engineering (OptumG2). Computer software*. Retrieved from https://www. optumce.com.

Вплив тріщинуватого матеріалу на стійкість тунелю (чисельне дослідження)

Талеб Хосні Абдеррахман[*1,2], *Гуеміді Ісмахене*[1,3]

1 – Лабораторія надійності матеріалів і конструкцій, Університет Бешара, м. Бешар, Алжир
2 – Кафедра цивільного будівництва та гідравліки, Інститут науки і технологій, Університетський центр Міла, м. Міла, Алжир
3 – Університет Чадлі Бенджедід, м. Ель-Тарф, Алжир
* Автор-кореспондент e-mail: talebhosni@yahoo.fr

Мета. Зрозуміти вплив тріщинуватого матеріалу на тунелі. Ці тунелі інфраструктури повинні бути безпечними в усіх відношеннях, включаючи будівництво, матеріали та інше. Одна із труднощів, з якою стикаються інженери, полягає в тому, що необхідно враховувати типи матеріалів, а також матеріал із тріщинами. У результаті, щоб забезпечити безпеку тунелю, нам важливо передбачати можливі опади, зміщення, напруги й деформації, викликані будівництвом тунелів у тріщинуватих середовищах.

Методика. Для даного чисельного дослідження використовувалося програмне забезпечення OPTUMG2, тунель моделювався з використанням гіпотези про двовимірну плоску деформацію за допомогою методу кінцевих елементів, що використовується для моделювання сцільних середовищ. Для моделювання пружнопластичної нелінійної поведінки цієї моделі використано критерій Мора-Кулона.

Результати. Отримані дані показують, що орієнтація площин ослаблення може мати значний вплив на стійкість тунелю. Так, було помічено, що 45 та 60° для кута α_1, а також 110 та 135° для другого кута α_2 являють собою найбільш критичні ситуації. Слід ураховувати вплив тріщинуватого матеріалу (ґрунту) на проекти цивільного будівництва, такі як проходження тунелів.

Наукова новизна. Стійкість тунелю визначається величиною переміщень (осідань), напруг і деформацій за наявності тріщин у навколишньому середовищі. У даній роботі ми змоделювали модель із різними кутами нахилу тріщин. Щодо орієнтації площини, для кута α_1 значення змінені на 0, 20, 45, 65 та 90°, другий кут α_2 змінювався від 110, 135, 155, 175 до 180°.

Практична значимість. Кількість тунелів та інфраструктурних проектів постійно збільшується. Це пов'язано з тим, що вони важливі для розвитку країн і прискорення економічного зростання, скорочення відстаней і часу в дорозі за рахунок з'єднання міських районів, в яких є природні перешкоди, такі як гори. Ми виявили, що площини орієнтації тріщин можуть мати великий вплив на стійкість тунелю. Так, було помічено, що 45 і 60° для першого кута та 110 і 135° для другого кута являють собою найбільш критичні ситуації.

Ключові слова: *моделювання тунелю, тріщинуватий матеріал, метод кінцевих елементів, осадка ґрунту, програма OPTUMG2*

The manuscript was submitted 30.05.22.